Date of publication xxxx 00, 0000, date of current version xxxx 00, 0000.

Digital Object Identifier

A Joint Beamforming and Power-splitter Optimization Technique for SWIPT in MISO-NOMA System

HAITHAM AL-OBIEDOLLAH[1], (Member, IEEE), KANAPATHIPPILLAI CUMANAN[2], (Senior Member, IEEE), HAYTHEM BANY SALAMEH[3,4], (Senior Member, IEEE), SANGARAPILLAI LAMBOTHARAN[5], (Senior Member, IEEE), YOGACHANDRAN RAHULAMATHAVAN[6], (Senior Member, IEEE), ZHIGUO DING [7], (Fellow, IEEE), and OCTAVIA A. DOBRE [8], (Fellow, IEEE)

[1]Department of Electrical Engineering, The Hahsemite University, Zarqa 13133, Jordan, (email:haithamm@hu.edu.jo)
[2]Department of Electronic Engineering, University of York, York, YO10 5DD, UK. (Email: kanapathippillai.cumanan@york.ac.uk.)
[3] Department of Communications and Networking, Al Ain University, Al Ain, UAE (Email: haythem.banysalameh@aau.ac.ae)
[4] Telecommunications Engineering Department, Yarmouk University, 22163 Irbid, Jordan
[5]Wolfson School of Mechanical, Electrical and Manufacturing Engineering, Loughborough University, Loughborough LE11 3TU, U.K (Email:S.Lambotharan@lboro.ac.uk)
[6]Institute for Digital Technologies, Loughborough University, London E15 2GZ, UK. (Email: Y.Rahulamathavan@lboro.ac.uk)
[7] School of Electrical and Electronic Engineering, The University of Manchester, Manchester, UK. (Email: zhiguo.ding@manchester.ac.uk)
[8] Department of Electrical and Computer Engineering, Memorial University, St. John's, NL A1B 3X5, Canada (email: odobre@mun.ca)

Corresponding author: H. AL-OBIEDOLLAH (e-mail: haithamm@hu.edu.jo).

This work was supported by the U.K.–India Education Research Initiative (UKIERI) under Grant UGC-UKIERI-2016-17-019. The work of Octavia A. Dobre was supported in part by the Natural Sciences and Engineering Research Council of Canada (NSERC) through its Discovery program.

ABSTRACT In this paper, we propose a joint beamforming and power-splitter optimization technique for simultaneous wireless power and information transfer in the downlink transmission of a multiple-input single-output (MISO) non-orthogonal multiple access (NOMA) system. Accordingly, each user employs a power splitter to decompose the received signal into two parts, namely, the information decoding and energy harvesting. The former part is used to decode the corresponding transmitted information, whereas the latter part is utilized for harvesting energy. For this system model, we solve an energy harvesting problem with a set of design constraints at the transmitter and the receiver ends. In particular, the beamforming vector and the power splitting ratio for each user are *jointly* designed such that the overall harvested power is maximized subject to minimum per-user rate requirements and the available power budget constraints at the base station. As the formulated problem turns out to be non-convex in terms of the design parameters, we propose a sequential convex approximation technique and demonstrate a superior performance compared to a baseline scheme.

INDEX TERMS Non-orthogonal multiple access (NOMA), energy harvesting, simultaneous wireless power and information transfer (SWIPT).

I. INTRODUCTION

RECENTLY, non-orthogonal multiple access (NOMA) has been identified as a promising multiple access technique to meet the unprecedented data rate requirements in the fifth generation (5G) and beyond [1]. In the downlink transmission of power-domain NOMA, multiple users can be served in the same orthogonal resources (time and frequency) through employing superposition coding at the transmitter [2] [3] [4]. At the receiver ends, users with stronger channel conditions exploit successive interference cancellation (SIC) by detecting and subtracting the signals intended to the users with weaker channel conditions [5] [6]. Due to its potential benefits and capabilities, NOMA has been incorporated with different spatial multiplexing techniques to facilitate its implementation in dense networks, while further improving the spectral efficiency [7]. These techniques include multiple-input multiple-output (MIMO) [8] [9] [10], and multiple-input single-input systems (MISO) [11] [12] [13]. These NOMA integrated systems are considered as potential solutions to provide massive connectivity in 5G and beyond while

supporting the proliferation of Internet-of-Things (IoT) [14].

With the explosive growth of data traffic and number of devices, the environmental and economical concerns associated with the power consumption have become one of the major issues that need to be carefully addressed in the development of new technologies [15]. Among various research directions, one of the promising solutions considered in the literature is the efficient utilization of the available power resources to maximize the overall energy efficiency (EE) of the communication systems [16] [17]. This EE maximization approach provides the flexibility to strike a good balance between the achieved data rate of a system and the corresponding power consumption [16]. Secondly, owing to the fact that non-green power resources have undesirable impacts on both environment and economy, recent solutions promote to employ the green renewable energy resources including wind and solar power [15]. Particularly, recent research activities have focused on the novel energy harvesting technique with simultaneous wireless power and information transfer (SWIPT) technology. This technology has been identified as one of the potential solutions to address the excessive power consumption issues in future wireless networks [18] [19].

The underlying concept of SWIPT is to utilize the RF signal to simultaneously transmit information and energy through the wireless medium [19] [20]. Theoretically, this can be accomplished by decomposing the received signal into two parts at the receiver end, namely, information decoding (ID) and energy harvesting (EH) [21]. This decomposition is performed by employing either the power splitting (PS) technique or the time switching technique (TS) [22]. Although, the PS techniques impose additional hardware complexity at the receiver end, it is preferred over TS techniques due to flexibility of practical implementations [21] [22]. This is due to the fact that TS demands a tight synchronization between the transmitter and receiver [23] [24]. Furthermore, the receiver requires the perfect instantaneous timing information for the EH and ID, which is challenging to achieve in practice, especially in real-time delay-tolerant applications. SWIPT is expected to play a crucial role in future generations of wireless networks. We provide a brief discussion on some of its applications. Firstly, SWIPT has the potential to wirelessly charge various medical sensors inside a human body which will avoid any need for physical wired connections. Replacing or charging these medical sensors is either expensive or even impractical due to invasive surgery requirements [25]. The SWIPT technology will become a potential way of providing power supply to wireless-powered sensor networks (WPSN) such as those deployed in buildings for structural monitoring [26]. Furthermore, SWIPT can be a viable solution for providing power supply for satellite communication systems [25] [26]. In particular, satellites can simultaneously transmit power and information for low-power-consumed mobile base stations including unmanned aerial vehicles [26]. Furthermore, EH through SWIPT can be utilized to provide power supply for the satellites [26] [27]. In cooperative networks, the EH through SWIPT can enhance the performance of users with weaker channel conditions [28] [29]. In addition, SWIPT can be an essential energy source in low-power IoT wireless systems, where a large number of energy-hungry devices with the limitation of battery size has to be always charged to support different wireless applications and services [30] [31]. In fact, SWIPT is an appealing solution to extend billions of IoT devices' lifetime while achieving self-sustainability [32] [33] [34]. Hence, EH through SWIPT would undoubtedly make fundamental impacts on the future green communications [35].

A. LITERATURE REVIEW

In order to fully exploit the potential benefits offered by the combined NOMA and SWIPT, several research studies have been performed recently. In particular, different resource allocation techniques have been proposed for SWIPT-based NOMA systems to realize their capabilities. For example, the authors in [36] have considered a single-input single-output (SISO) TS-based SWIPT system in which time and power are jointly allocated to maximize the overall EE of the system with minimum-rate and minimum harvested-power constraints. Furthermore, a sum-rate maximization problem for SWIPT-based MISO-NOMA system has been considered in [37], where the users could either harvest energy or receive the corresponding information. Similarly, the authors in [38] have considered the sum-rate maximization for a SWIPT-based MISO-NOMA system with a PS approach where two users are grouped into a cluster. In each cluster, the near-user has the potential to simultaneously harvest energy and decode information, whereas the weaker user can decode only its corresponding information. In [39], a power minimization problem has been considered for a SWIPT-based MISO-NOMA cognitive network. Robust beamforming algorithms for maximizing the weighted sum rate and for minimizing the total power consumption have been investigated in [40]. A *cooperative* transmission of SWIPT based MISO-NOMA has been considered in the downlink in [41]. In this cooperative communication scenario, the stronger users utilize the harvested energy to forward the signals of the weaker users after decoding them through SIC [41] [42]. In fact, the strong users operate as relays to further improve the performance of the weaker users.

B. CONTRIBUTIONS

In SWIPT, the received RF signal, including both the useful and the interference components, is utilized to harvest energy. In particular, undesired interference is converted into a useful resource in SWIPT-based communication systems [29]. The SWIPT technology perfectly aligns with the fundamental concept of NOMA as the users are served by sharing the same orthogonal resources [43]. This non-orthogonal resource sharing introduces more interference at the receivers com-

pared to that of the conventional orthogonal multiple access systems. The additional interference can be exploited to harvest energy with SWIPT technology. Therefore, SWIPT perfectly suits the NOMA systems for offering complementary benefits to the users [3]. Furthermore, the interference and the additional degrees of freedom with multiple-antenna techniques can also support the core concept of SWIPT [44]. Motivated by the promising capabilities of combining a multi-antenna NOMA system with the SWIPT technique, we consider a SWIPT based MISO-NOMA system. For this system model, we propose a joint beamforming and power-splitting optimization technique for a *non-cooperative* transmission of SWIPT based MISO-NOMA system. In particular, the EH capabilities of the MISO-NOMA system are considered with users having the ability to decode information and harvest energy simultaneously. This scenario perfectly aligns with the requirements of WPSN, in which a set of sensors demands to be always charged through maximizing the harvested energy while achieving minimum-rate constraints [25]. The developed optimization problem turns out to be non-convex in its original form. Hence, a sequential convex approximation (SCA) is adopted to tackle this non-convexity issue. Additionally, we investigate the feasibility of the problem prior to solving it. Furthermore, we investigate the efficiency of the proposed SCA technique by evaluating its performance. The performance of the proposed MISO-NOMA beamforming design is evaluated versus a baseline MISO system with zero forcing beamforming (ZFBF) in terms of the overall harvested energy [45].

The remainder of the paper is organized as follows. Section II introduces the system model of a SWIPT based MISO-NOMA system and formulates the harvested power maximization problem. Section III provides the technical details of the proposed algorithms to examine the feasibility and present the solution of the original optimization problem. Section IV presents simulation results, which demonstrate the effectiveness of the proposed beamforming design and evaluate its performance versus a baseline design. Finally, conclusions are drawn in Section V.

C. NOTATIONS

We use lower case boldface letters for vectors and upper case boldface letters for matrices. $(\cdot)^H$ denotes complex conjugate transpose. $\Re(\cdot)$ and $\Im(\cdot)$ stand for real and imaginary parts of a complex number, respectively. The symbols $\mathbb{C}^N$ and $\mathbb{R}^N$ denote N-dimensional complex, and real spaces, respectively. $||\cdot||_2$ and $|\cdot|$ represent the Euclidean norm of a vector and absolute value of a complex number, respectively.

II. SYSTEM MODEL AND PROBLEM FORMULATION

A. SYSTEM MODEL

We consider the downlink transmission of a MISO-NOMA system, in which a BS with N transmit antennas communicates simultaneously with all K single-antenna users. Each user performs energy harvesting and decoding as shown in

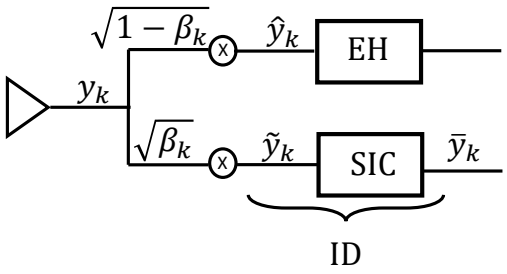

FIGURE 1: SWIPT receiver with PS technique.

Fig. 1. The BS encodes the symbol intended to each user by multiplying with its corresponding beamforming vector. Therefore, the transmitted signal from the BS is given by

$$\mathbf{x} = \sum_{i=1}^{K} \mathbf{b}_i s_i, \tag{1}$$

where s_i and $\mathbf{b}_i \in \mathbb{C}^{N\times 1}$ denote the symbol intended for the i^{th} user (U_i) and the corresponding beamforming vector, respectively. The received signal at U_k can be written as

$$y_k = \mathbf{h}_k^H \sum_{j=1}^{K} \mathbf{b}_j s_j + n_k, \tag{2}$$

where n_k is zero mean circularly symmetric complex additive white Gaussian noise (AWGN) with variance σ_i^2, while $\mathbf{h}_k \in \mathbb{C}^{N\times 1}$ represents the channel vector between the BS and U_k. This channel vector can be expressed as

$$\mathbf{h}_k = (\frac{1}{d_k})^{\phi} \mathbf{g_k}, \tag{3}$$

where d_k denotes the distance (in meter) between the BS and U_k, ϕ is the path loss exponent, $\mathbf{g_k}$ represents the small scale fading coefficient, assumed to be complex-valued normal distributed with zero mean and unity variance. Furthermore, we assume that each user has a power splitter such that a fraction (β_k) of y_k is utilized to decode the data in the ID stage, i.e., $0 \leq \beta_k \leq 1$. In addition, the fraction $(1-\beta_k)y_k$ is used to harvest the energy through the EH circuit, as depicted in Fig. 1. We provide further details of the PS technique in the following discussions.

ID Stage

The signal at the output of the ID stage $\tilde{y}_k$ is given as $\tilde{y}_k = \sqrt{\beta} y_k + \tilde{n}_k$, where y_k is corrupted by the AWGN $\tilde{n}_k$. This noise is due to processing of y_k in the ID circuit [21]. In particular, $\tilde{n}_k$ is AWGN with variance $\tilde{\sigma}_k^2$. Based on the fundamental concepts of NOMA, the users with stronger channel conditions have the capability to decode and subtract the signals intended for the weaker users through employing SIC [46]. Therefore, users' ordering based on the channel conditions is a crucial factor which significantly influences

the performance of NOMA systems. Based on this key fact, we order the users such that U_1 has the strongest channel condition, whereas U_K has the weakest channel condition. This can be expressed as follows:

$$||\mathbf{h}_1||_2^2 \geq ||\mathbf{h}_2||_2^2 \geq \cdots \geq ||\mathbf{h}_K||_2^2. \quad (4)$$

Following this user ordering in (4), U_k has the capability to sequentially decode and subtract the symbols of the weaker users $U_{k+1}, U_{k+2} \cdots U_K$, prior to decoding its own signal. The user U_k performs SIC by firstly decoding the signal of the weakest user, and then subtracts the corresponding portion of the received signal. Hereafter, the stronger users refer to the users with stronger channel conditions. This SIC process is continued with the other weaker users (i.e., $U_{K-1}, \cdots, U_{k+1}, U_k$) until y_{k+1} is correctly decoded and subtracted from the received signal [47] [2]. Then, U_k decodes its own signal, and the received signal at U_k after employing SIC technique with other weaker users can be written as

$$\bar{y}_k = (\sqrt{\beta_k})\,(\mathbf{h}_k^H \sum_{i=1}^{k-1} \mathbf{b}_i s_i + n_k) + \tilde{n}_k. \quad (5)$$

The received signal-to-noise and interference ratio (SINR) of the decoding signal intended for the weaker user U_j, i.e., $j \geq k$, at U_k (SINR_j^k) can be written as

$$\text{SINR}_j^k = \frac{\beta_k |\mathbf{h}_k^H \mathbf{b}_j|^2}{\beta_k (\sum_{z=1}^{j-1} |\mathbf{h}_k^H \mathbf{b}_z|^2 + \sigma_k^2) + \hat{\sigma}_k^2}, \; \forall k \in \mathcal{K}. \quad (6)$$

Note that $\mathcal{K} = \{1, 2, \cdots, K\}$ defines the set of all users. Furthermore, the signal of U_j is successfully decoded at $U_1, U_2 \cdots U_j$ if-and-only-if the SINR of decoding this signal is larger than a certain pre-defined threshold. Then, this should be satisfied at all other stronger users in order to correctly decode the signal. As a result [2],

$$\text{SINR}_j = \min \{\text{SINR}_j^k\}_{k=1}^j, \forall j \in \mathcal{K}. \quad (7)$$

Note that the SIC process could not be practically implemented unless the SINR of the decoding signal intended for the weaker user signal at U_k (SINR_j^k) is higher than that of the stronger users. This can be guaranteed by imposing the following constraints [48]:

$$|\mathbf{h}_k^H \mathbf{b}_K|^2 \geq |\mathbf{h}_k^H \mathbf{b}_{K-1}|^2 \geq \cdots | \geq |\mathbf{h}_k^H \mathbf{b}_1|^2, \forall k \in \mathcal{K}. \quad (8)$$

It is worth mentioning that the constraint in (8) is referred to as SIC constraint in the literature.

With this successful implementation of SIC, the achieved rate at U_j can be expressed as

$$R_j = B_w \log(1 + \text{SINR}_j), \forall j \in \mathcal{K}, \quad (9)$$

where B_w denotes the available bandwidth. Additionally, the achieved sum rate of the system can be defined as

$$R = \sum_{j=1}^{K} R_j. \quad (10)$$

EH Stage

The EH circuit utilizes the EH part to harvest energy at the EH stage. The received signal after EH stage can be written as

$$\hat{y}_k = \sqrt{1 - \beta_k} y_k + \hat{n}_k, \quad (11)$$

where $\hat{n}_k$ is the AWGN with zero mean and variance $\hat{\sigma}_k^2$ introduced by the processing of y_k in the EH stage. The EH circuit mainly consists of a matching network, a radio frequency to direct current (RF-DC) and a storage unit [24]. By ignoring the noise power (i.e., $\hat{\sigma}_k^2$ and σ_k^2) [49], the harvested power at U_k can be expressed as [50]

$$\text{P}_{k,H} = \eta \sum_{i=1}^{K} (1 - \beta_k) |\mathbf{h}_k^H \mathbf{b}_i|^2, \quad (12)$$

where η denotes the efficiency of the RF-DC converter in the EH stage. It is worth mentioning that the practical experiments reveal that the harvested energy first grows almost linearly with the input power, and then saturates when the input power reaches to a certain level [50] [51]. In fact, several models have been considered to reflect such non-linear characteristics of the EH circuit, including non-linear EH (NL-EH) model based on the logistic (sigmoid) function [40]. In particular, it was shown that the non-linear model can provide higher performance gain than that of the linear model [52], [53]. As such, the performance gains of linear EH model can be viewed as a benchmark performance for the techniques developed with non-linear EH model. To this end, a linear model is considered in this paper to establish a benchmark performance. Hence, the overall harvested power by all the users in the above MISO-NOMA system can be written as

$$\text{P}_H = \eta \sum_{k=1}^{K} \sum_{i=1}^{K} (1 - \beta_k) |\mathbf{h}_k^H \mathbf{b}_i|^2. \quad (13)$$

Note that the total harvested energy at all users can be defined as

$$\text{E}_H = T(\eta \sum_{k=1}^{K} \sum_{i=1}^{K} (1 - \beta_k) |\mathbf{h}_k^H \mathbf{b}_i|^2), \quad (14)$$

where T denotes the transmission time. [1] It is worth pointing out that our analysis is performed based on the harvested power.

B. PROBLEM FORMULATION

We investigate the energy harvesting capabilities of the MISO-NOMA system. A joint design of the beamforming vectors $\{\mathbf{b}_i\}_{i=1}^K$ and the PS ratios $\{\beta_i\}_{i=1}^K$ is considered to maximize the harvested power P_H with a minimum-rate requirement at each user, referred to as R_k^{min}. This requirement ensures that the received power is shared between ID and EH instead of being fully used for EH. It is worth mentioning that the ignorance of this constraint leads to a significant

[1] In this paper, T is assumed to be one, and thus, energy and power carry the same meaning.

degradation in the achieved rate at the corresponding user. This minimum rate requirement can be formulated as the following constraint in terms of SINR:

$$\text{SINR}_k \geq \text{SINR}_k^{min}, \ \forall k \in \mathcal{K}, \tag{15}$$

where $\text{SINR}_k^{min} = 2^{\text{R}_k^{min}} - 1$. Furthermore, the beamforming design should consider the available power budget at the BS, P^A, which can be defined through the following constraint:

$$\sum_{k=1}^{K} ||\mathbf{b}_k||_2^2 \leq \text{P}^A. \tag{16}$$

With the above constraints and the SIC constraints in (8), the design parameters (i.e., $\{\beta_i\}_{i=1}^K$ and $\{\mathbf{b}_i\}_{i=1}^K$) can be determined by solving the following optimization problem:

$$OP_H\text{: } \underset{\{\mathbf{b}_k,\beta_k\}_{k=1}^K}{\text{maximize}} \quad \eta \sum_{k=1}^{K}\sum_{i=1}^{K}(1-\beta_k)|\mathbf{h}_k^H\mathbf{b}_i|^2 \tag{17a}$$

$$\text{subject to} \quad \text{SINR}_k \geq \text{SINR}_k^{min}, \ \forall k \in \mathcal{K}, \tag{17b}$$

$$\sum_{k=1}^{K} ||\mathbf{b}_k||_2^2 \leq \text{P}^A, \tag{17c}$$

$$(8). \tag{17d}$$

There are a number of challenges associated with solving the optimization problem OP_H defined in (17). First, the feasibility of the problem should be examined prior to solving OP_H to ensure that the required minimum-rates can be achieved with the given power budget. The second challenge is the non-convexity of the objective function and the constraints in (17b) and (17d). This means that OP_H is a non-convex optimization problem, which could not be directly solved via available software. Finally, once the problem is solved, an evaluation process has to be carried out to verify the effectiveness of the obtained solution. With these challenges, we develop a comprehensive methodology to determine a feasible solution in the following section.

III. THE PROPOSED METHODOLOGY

In this section, we first examine the feasibility of the optimization problem OP_H. Then, we propose an efficient algorithm to solve the problem OP_H and determine the design parameters, i.e., $\{\mathbf{b}_i, \beta_i\}_{i=1}^K$. Finally, we evaluate the effectiveness of the proposed approach through numerical simulations.

A. FEASIBILITY OF OP_H

It is apparent that the optimization problem OP_H is only feasible when the available power budget (i.e., P^A) is sufficient to achieve the minimum rate requirements of all users. Otherwise, the problem becomes infeasible. Once the feasibility of the optimization problem is verified, it can be solved. In order to examine the feasibility, we first assume that all the users are completely switched to ID mode (i.e., $\beta_i = 1, \ \forall i$). Then, we evaluate the corresponding required minimum transmit power (P_t^{min}) to meet the minimum rate requirements. In this setting, when P_t^{min} exceeds P^A, the harvested power maximization problem OP_H turns out to be infeasible. As such, we evaluate P_t^{min} through solving the following power minimization (P-Min) problem:

$$OP_P\text{: } \text{P}_t^{min} = \underset{\{\mathbf{b}_i\}_{i=1}^K}{\text{minimize}} \quad \sum_{k=1}^{K} ||\mathbf{b}_i||_2^2 \tag{18a}$$

$$\text{subject to} \quad \text{SINR}_k \geq \text{SINR}_k^{min}, \ \forall k \in \mathcal{K}, \tag{18b}$$

$$(8). \tag{18c}$$

Note that OP_P was solved in [8], however, the solution of this non-convex problem can be found throughout this paper. If $\text{P}_t^{min} \leq \text{P}^A$, then the optimization problem OP_H is obviously feasible and worthy to solve at least under the worst-case scenario, i.e., the users can achieve their minimum rate requirements without EH. On the other hand, if $\text{P}_t^{min} > \text{P}^A$, then OP_H becomes infeasible and cannot be solved with the available power budget. In this case, the BS has two choices: either to notify the users that the available power budget cannot support their minimum rate requirements and does not transmit, or to maximize the sum rate of all users without considering the minimum rate requirements. In this work, we alternatively design the beamforming vectors to maximize the sum rate for the case of $\text{P}_t^{min} > \text{P}^A$. These beamforming vectors can be determined through solving the following sum-rate maximization (SRM) problem:

$$OP_R\text{: } \underset{\{\mathbf{b}_i\}_{i=1}^K}{\text{maximize}} \quad \sum_{k=1}^{K} \text{R}_k \tag{19a}$$

$$\text{subject to} \quad \sum_{i=1}^{K} ||\mathbf{b}_i||_2^2 \leq \text{P}^A, \tag{19b}$$

$$(8). \tag{19c}$$

Note that the solution of the SRM problem OP_R can be found in the context of this paper, whereas the full detailed solution is available in [48] [54].

B. THE PROPOSED ALGORITHM TO SOLVE OP_H

We consider a feasible optimization problem OP_H and its feasibility can be validated through the feasibility check introduced earlier in this section. Thus, it is worthy to solve the feasible OP_H. However, there are a number of issues that needs to be addressed before solving OP_H, including the non-convexity, the joint design of the beamforming vectors, and the PS ratio. In particular, the OP_H in (17) is a non-convex problem due to the non-convex objective function and the constraints in (17b) and (17d), respectively. Therefore, the non-convex optimization problem OP_H cannot be solved directly using the existing software. We deal with these non-convexity issues by developing an iterative algorithm based on the SCA technique. In this SCA algorithm, each non-convex term is approximated with a lower convex-concave (linear) approximation using the first-order Taylor series, and

the original optimization problem is iteratively solved [55]. In particular, the SCA algorithm has been widely utilized to solve several resource allocation problems in the literature [56] [57], [58] and [47]. We start handling the non-convexity of the objective function of OP_H by decomposing it into two parts: $\sum_{i=1}^{K}(1-\beta_k)$ and $|\mathbf{h}_k^H\mathbf{b}_i|_2^2$. Then, each part is bounded by a slack variable as follows:

$$|\mathbf{h}_k^H\mathbf{b}_i|^2 \geq \alpha_{k,i}, \forall k \in \mathcal{K}, \forall i \in \mathcal{K}, \tag{20a}$$
$$1-\beta_k \geq \Gamma_k^2, \forall k \in \mathcal{K}. \tag{20b}$$

With these new slack variables, we define the objective function in OP_H as follows:

$$\Gamma_k^2\alpha_{i,k} \geq \chi_{i,k}, \forall k \in \mathcal{K}, \forall i \in \mathcal{K}. \tag{21}$$

Without loss of generality, the objective function of OP_H can be equivalently expressed as

$$(17a) \Leftrightarrow \begin{cases} \text{maximize} & \eta\sum_{k=1}^{K}\sum_{i=1}^{K}\chi_{i,k} & (22a) \\ \text{subject to} & (20a),(20b),(21). & (22b) \end{cases}$$

Obviously, the non-convex objective function in the original problem OP_H has been replaced by the lower bounded slack variable $\chi_{i,k}$. However, the non-convex constraints (20a), (20b), and (21) are now included in OP_H. Therefore, we handle these non-convex constraints in the following discussion. In fact, the non-convexity of (20a) can be handled by approximating its left-hand side with a lower convex-concave (linear) expression using the first-order Taylor series as follows:

$$\alpha_{i,k}^{(t+1)} \geq \left|\left|\left[\varrho_{i,k}^{(t)} \ , \ \rho_{i,k}^{(t)}\right]\right|\right|_2^2 + 2\left[\varrho_{i,k}^{(t)} \ , \ \rho_{i,k}^{(t)}\right]^T\left[\varrho_{i,k}^{(t+1)}-\varrho_{i,k}^{(t)} \ , \ \rho_{i,k}^{(t+1)}-\rho_{i,k}^{(t)}\right], \tag{23}$$

where

$$\varrho_{i,k}^{(t)} = \Re\{\mathbf{h}_i^H\mathbf{b}_k^{(t)}\}, \forall k \in \mathcal{K}, \forall i \in \mathcal{K}, \tag{24a}$$
$$\rho_{i,k}^{(t)} = \Im\{\mathbf{h}_i^H\mathbf{b}_k^{(t)}\}, \forall k \in \mathcal{K}, \forall i \in \mathcal{K}. \tag{24b}$$

Note that the superscript $(\cdot)^{(t)}$ denotes the approximation at the t^{th} iteration Similarly, the non-convexity of the constraint in (20b) can be handled using the same technique that was utilized for the previous constraint. With this approximation, the non-convex constraint in (20b) can be equivalently written as

$$1-\beta_k \geq \Gamma_k^{2\,(t)} + 2\Gamma_k^{(t)}(\Gamma_k^{(t+1)}-\Gamma_k^{(t)}). \forall k \in \mathcal{K}. \tag{25}$$

Now, we approximate the left side of the inequality (21) as follows:

$$\Gamma_k^{2\,(t)}\alpha_{i,k}^{(t)} + \Gamma_k^{2\,(t)}\left(\alpha_{i,k}^{(t+1)}-\alpha_{i,k}^{(t)}\right) + 2\Gamma_k^{(t)}\alpha_{i,k}^{(t)}\left(\Gamma_k^{(t+1)}-\Gamma_k^{(t)}\right) \geq \chi_{i,k}, \forall k \in \mathcal{K}, \forall i \in \mathcal{K}. \tag{26}$$

To summarize, we have replaced the non-convex objective function of OP_H by the convex slack variable, (22a), subject to the convex constraints provided in (23), (25), and (26).

Next, we handle the non-convex constraints in (17b) and (17d) in the original OP_H problem. By introducing the slack variable κ_k, the minimum SINR constraint in (17b) can be decomposed into a set of constraints as follows:

$$\beta_i|\mathbf{h}_i^H\mathbf{b}_k|^2 \geq \gamma_k\kappa_k^2, \ \forall k, i \leq k, \tag{27a}$$
$$\kappa_k^2 \geq \beta_i(\sum_{z=1}^{k-1}|\mathbf{h}_i^H\mathbf{b}_z|^2 + \sigma_i^2) + \hat{\sigma}_i^2, \forall k, i \leq k, \tag{27b}$$

where $\gamma_k = \text{SINR}_k^{min}$. The non-convexity of the constraint in (27a) can be handled through incorporating new slack variables, namely Υ_j and $\varpi_{i,k}$, such that this constraint can be reformulated as the following set of constraints:

$$\beta_i \geq \Upsilon_i^2, \quad \forall i, \tag{28a}$$
$$\Upsilon_i^2\alpha_{k,i} \geq \varpi_{k,i}, \quad k \in \mathcal{K}, i \leq k, \tag{28b}$$
$$\varpi_{k,i} \geq \gamma_k\kappa_k^2, \quad k \in \mathcal{K}, i \leq k. \tag{28c}$$

By reformulating each non-convex term with a linear approximation using the first-order Taylor series, the non-convex constraints in (28) can be transformed into the following convex constraints:

$$\beta_i \geq \Upsilon_i^{2\,(t)} + 2\Upsilon_i^{(t)}(\Upsilon_i^{(t+1)}-\Upsilon_i^{(t)}), \forall i, \tag{29a}$$
$$\Upsilon_i^{2\,(t)}\alpha_{k,i}^{(t)} + \Upsilon_i^{2\,(t)}\left(\alpha_{k,i}^{(t+1)}-\alpha_{k,i}^{(t)}\right) + 2\alpha_{k,i}^{(t)}\Upsilon_i^{(t)}\left(\Upsilon_i^{(t+1)}-\Upsilon_i^{(t)}\right) \geq \varpi_{k,i}, k \in \mathcal{K}, i \leq k, \tag{29b}$$
$$\varpi_{k,i} \geq \gamma_k\left(\kappa_k^{2\,(t)} + 2\kappa_k^{(t)}(\kappa_k^{(t+1)}-\kappa_k^{(t)})\right), k \in \mathcal{K}, i \leq k. \tag{29c}$$

Similarly, the non-convex constraint in (27b) can be approximated by the following convex constraint:

$$\kappa_k^{2\,(t)} + 2\kappa_k^{(t)}(\kappa_k^{(t+1)}-\kappa_k^{(t)}) \geq \sum_{z=1}^{k-1}\varpi_{i,z} + \sigma_i^2\left(\Upsilon_i^{2\,(t)} + 2\Upsilon_i^{(t)}(\Upsilon_i{}^{(t+1)}-\Upsilon_i{}^{(t)})\right) + \hat{\sigma}_i^2, k \in \mathcal{K}, i \leq k. \tag{30}$$

Based on the above approximations, the non-convex constraint in (17b) is transformed into the following set of convex constraints:

$$(17b) \Leftrightarrow (29a),(29b),(29c),(30). \tag{31}$$

Finally, the SIC constraint in (17d) can be formulated as a convex one by replacing each term in the inequality by the lower slack variable $\alpha_{i,k}$. Therefore, this constraint can be written as

$$\alpha_{k,K} \geq \alpha_{k,K-1} \geq \cdots \geq \alpha_{k,1}, \ \forall k \in \mathcal{K}. \tag{32}$$

With these multiple slack variables, the approximated convex form of the original non-convex problem OP_H can be defined as follows:

$$\begin{aligned} \hat{OP}_H: \underset{\Pi}{\text{maximize}} \quad & \eta \sum_{k=1}^{K} \sum_{i=1}^{K} \chi_{i,k} \\ \text{subject to} \quad & (17c), (23), (25), \\ & (26), (31), (32), \end{aligned}$$

where Π includes all the design parameters, such that $\Pi = \{\mathbf{b}_k, \alpha_{j,k}, \Upsilon_k, \Gamma_k, \kappa_k, \beta_k, \varrho_{j,k}, \rho_{j,k}, \chi_{j,k}, \varpi_{i,k}\}_{k=1}^{K}$.

It is clear that the optimization problem $\hat{OP}_H$ is iteratively solved, such that the obtained solutions at the t^{th} iteration are used as initialization for the next $t+1^{th}$ iteration. Considering this iterative algorithm, three important issues need to be clearly addressed. First, the iterative algorithm based solution requires appropriate selection of the initial parameters, i.e., $\Pi^{(0)}$. Note that a random selection of the initial parameters might make the $\hat{OP}_H$ infeasible. The inappropriate selection of initial parameters has a direct impact on the convergence speed of the iterative algorithm. Secondly, with this SIC algorithm, the solution is obtained and the algorithm is terminated when the difference between two successive solutions is less than a pre-defined accuracy. Finally, as the original non-convex optimization problem OP_H is *approximated* by the convex one $\hat{OP}_H$, it is important to validate the effectiveness of the proposed iterative algorithm. All the above issues are addressed in the following subsections.

C. INITIALIZATION, COMPLEXITY ANALYSIS AND PERFORMANCE EVALUATION

1) Initial Parameters and Convergence

As highlighted in the previous subsection, an inappropriate selection of the initial parameters $\Pi^{(0)}$ for the proposed SCA algorithm might make the original problem infeasible and not provide a solution. Therefore, we present a systematic approach to select the initial parameters. As such, the beamforming vectors obtained through solving OP_P, $\{\mathbf{b}_i^{min}\}_{i=1}^{K}$, are utilized to initialize the parameters, such as $\{\mathbf{b}_i^{(0)}\}_{i=1}^{K} = \{\mathbf{b}_i^{min}\}_{i=1}^{K}$. Consequently, all slack variables can be determined by substituting $\{\mathbf{b}_i^{(0)}\}_{i=1}^{K}$ at each inequality that defines the corresponding slack variables. For example, the initial slack variable $\alpha_{k,i}^{(0)}$ can be determined as follows:

$$\alpha_{k,i}^{(0)} = \mathbf{h}_k^H \mathbf{b}_i^{(0)}, \forall k, \forall i. \tag{34}$$

Additionally, this initialization not only ensures the feasibility of the proposed SCA algorithm, but also speeds up its convergence to yield a feasible solution. This will be confirmed through simulation results in Section IV. Note that the proposed iterative algorithm terminates when the absolute difference between two successive solutions is less than a pre-defined threshold ν. As such, the corresponding solution is denoted as $\Pi^{(*)}$. We summarize the proposed algorithm in Algorithm 1.

Algorithm 1 Harvested power maximization algorithm

Step 1: **F**easibility check examination.
1) Evaluate P_t^{min} through solving OP_P.
   a) If $\mathsf{P}_t^{min} > \mathsf{P}^A \Rightarrow OP_H$ is infeasible
      Find beamforming vectors that solve OP_R.
   b) If $\mathsf{P}_t^{min} \leq \mathsf{P}^A \Rightarrow OP_H$ is feasible
      Go to Step 2.

Step 2: Evaluating $\Pi^{(*)}$.
1) **I**nitialization (i.e., $\Pi^{(0)}$).
2) **R**epeat
   a) Solve the optimization problem $\hat{OP}_H$.
   b) Until the required accuracy is achieved.

Step 3: End of the Algorithm.

2) Complexity Analysis of the Proposed SCA Technique

The original optimization problem OP_H is solved using an iterative SCA algorithm, in which different approximations and slack variables are introduced. In particular, the solution of OP_H is obtained by iteratively solving the approximated convex optimization problem $\hat{OP}_H$. With linear objective function and constraints, the problem $\hat{OP}_H$ turns out to be a linear program which is solved using the Dantzig's simplex method [59]. Note that the number of arithmetic operations required to solve a linear program cannot be exactly defined; however, its complexity for one iteration is bounded by an order $\mathcal{O}(n^2 m)$, where m and n are the numbers of constraints and the optimization parameters, respectively [59]. Considering this, the complexity of solving the original optimization problem OP_H is bounded by $\mathcal{O}\left(n^2 m \log(\frac{1}{\nu})\right)$, where $m = K^3 + 6K^2 + K + 1$ and $n = 7K^2 + 5K$. Note that the computational complexity increases as the pre-defined threshold ν decreases.

3) Performance Validation

In this subsection, we discuss how to evaluate the performance of the proposed algorithm. This evaluation can be carried out by comparing the performance of the proposed algorithm with that that of an exhaustive search. However, note that the exhaustive search is not suitable for practical implementation due to its high computational complexity. Hence, we propose a novel approach to evaluate the performance of the proposed SCA algorithm. This approach can be summarized as follows:

- Firstly, by solving OP_H via the proposed SCA algorithm, we evaluate the harvested power at each user (i.e., $\mathrm{P}_{k,H}{}^{(*)}$), the power splitting ratio $\{\beta_k^{(*)}\}_{k=1}^{K}$, the beamforming vectors and the corresponding power allocations for all user ($\{P_k^{t(*)}\}_{k=1}^{K}$), such that $P_k^{t(*)} = ||\mathbf{b}_k{}^{(*)}||_2^2$.

- Next, we update OP_P by including the minimum harvested power constraints to the original P-Min problem in (18). These constraints are formulated as follows:

$$(1-\beta_k^*)\eta\sum_{j=1}^{K}\mathbf{h}_k^H\mathbf{b}_j \geq \mathrm{P}_{k,H}{}^{(*)}, \forall i \in \mathcal{K}. \tag{35}$$

With these additional constraints, the modified OP_P can be now defined as

$$\widetilde{OP}_P : \mathrm{P}_t^{min} = \underset{\{\mathbf{b}_i\}_{i=1}^K}{\text{minimize}} \sum_{k=1}^{K}||\mathbf{b}_i||_2^2 \tag{36a}$$

$$\text{subject to } \mathrm{SINR}_k \geq \mathrm{SINR}_k^{min},\ \forall k \in \mathcal{K}, \tag{36b}$$

$$(1-\beta_k^*)\eta\sum_{j=1}^{K}\mathbf{h}_k^H\mathbf{b}_j \geq \mathsf{P}_{k,H}{}^{(*)}, \forall i \in \mathcal{K}. \tag{36c}$$

$$(8). \tag{36d}$$

- Next, we reformulate $\widetilde{OP}_P$ in a semi-definite programming (SDP) form [60]:

$$\widetilde{\widetilde{OP}}_P : P^* =$$

$$\underset{\{\mathbf{B}_i\}_{i=1}^K}{\text{minimize}} \sum_{i=1}^{K}\mathrm{Tr}[\mathbf{B}_i] \tag{37a}$$

$$\text{subject to } \mathrm{Tr}[\mathbf{H}_k\mathbf{B}_i] - \gamma_i\sum_{j=1}^{i-1}\mathrm{Tr}[\mathbf{H}_k\mathbf{B}_j] \geq \gamma_i\sigma_k^2, \forall i \in \mathcal{K}, k \leq i, \tag{37b}$$

$$\mathrm{Tr}[\mathbf{H}_i\mathbf{B}_1] \leq \mathrm{Tr}[\mathbf{H}_i\mathbf{B}_2] \leq \cdots \leq \mathrm{Tr}[\mathbf{H}_i\mathbf{B}_K], \forall i \in \mathcal{K}, \tag{37c}$$

$$(1-\beta_k^*)\eta\sum_{j=1}^{K}\mathrm{Tr}[\mathbf{H}_k\mathbf{B}_j] \geq \mathsf{P}_{k,H}{}^{(*)} \tag{37d}$$

$$\mathbf{B}_i = \mathbf{B}_i^H, \mathbf{B}_i \succeq 0, \forall i \in \mathcal{K}, \tag{37e}$$

where $\mathbf{B}_i = \mathbf{b}_i\mathbf{b}_i^T$ and $\mathbf{H}_i = \mathbf{h}_i\mathbf{h}_i^T$. By relaxing rank-one constraints, referred to semi-definite relaxation in the literature, OP_P turns out to be a convex problem, and thus, the solution is optimal [61] [60] [62].
The optimal power allocation and the corresponding beamforming vectors obtained by solving $\widetilde{\widetilde{OP}}_P$ are denoted by $\{P_k^{t(**)}\}_{k=1}^K$ and $\{\mathbf{b}_k{}^{(**)}\}_{k=1}^K$, respectively.
- Finally, if the beamforming obtained through solving $\hat{OP}_H$ and $\widetilde{\widetilde{OP}}_P$ are similar, then, we can confirm that the iterative algorithm to solve the original non-convex optimization problem OP_H provides a near-optimal solution.

The simulation results confirm that the proposed algorithm with the SCA technique to solve OP_H yields a near-optimal solution with a small number of iterations.

IV. SIMULATION RESULTS

In this section, we evaluate the efficacy of the proposed technique and compare its performance against a baseline scheme. In particular, we examine the impacts of several parameters on the harvested power and verify the convergence of the proposed iterative algorithm. The CVX-package [63] is used to generate all the simulation results and the parameters considered in these simulations are summarized in Table 1. Note that for the numerical results, we have selected the simulation parameters the same as those in [41].

ZERO FORCING BEAMFORMING (ZFBF) BASELINE SCHEME

We use a ZFBF based transmission technique as a baseline scheme. For a ZFBF design with EH, the beamforming vector for each user and the corresponding PS ratio are determined such that overall harvested power is maximized [50]. The only requirement for such a system is that the number of transmit antennas should be equal to or less than the total number of users. Full details on this ZFBF design can be found in [49].

TABLE 1: Parameter values used in simulations.

Parameter	Value(s)
Number of users (i.e., K)	3
Transmit Antennas (i.e.,N)	3
User Distances	[30 20 10] (m)
Path Loss exponent (i.e., ϕ)	3.0
ID Noise Variance of Users (i.e., $\hat{\sigma_k^2}$), $\forall k$	-80 dBm/Hz
User Noise Variance of Users (i.e., σ^2), $\forall k$	-80 dBm/Hz
Threshold for Algorithm 1 (ν)	10^{-5}
RF-DC Efficiency (i.e., η)	0.8
Minimum SINR Thresholds (i.e., γ_k), $\forall k$	0 dB
Bandwidth (i.e.,B_w) (MHz)	1

Fig. 2 depicts the performance of the MISO-NOMA and ZFBF based MISO systems in terms of the harvested power. As seen, the MISO-NOMA system outperforms the conventional ZFBF based MISO system. This performance enhancement is due to the following two facts. Firstly, the beamforming vectors with the ZFBF design are orthogonal to each other and the co-channel interference introduced by combining the signals at the BS is completely eliminated. Therefore, this interference mitigation significantly degrades the EH capabilities of the ZFBF based MISO systems compared to the MISO-NOMA system. Secondly, the users in MISO-NOMA system exploit the co-channel interference through superposition coding and SIC to achieve a better performance. In fact, this enhances the EH capabilities at the receivers of the MISO-NOMA system where the users take advantage of the co-channel interference to harvest energy. For example, as seen in Fig. 2, with $\mathrm{P}^A = 20$ dB, the harvested power at the MISO-NOMA system is around 1 (i.e., $\mathrm{P}^H = 1$ Watt), whereas the harvested power is less than 0.4 Watt with the ZFBF design.

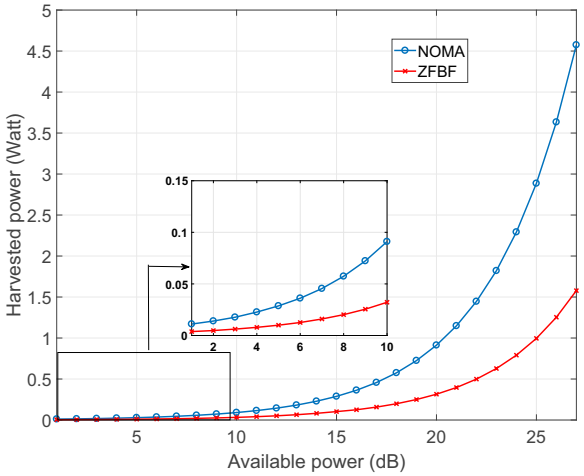

FIGURE 2: Harvested power of the MISO-NOMA system and the conventional ZFBF based MISO system against various available power levels.

Next, in Fig. 3, we demonstrate the impact of the minimum SINR requirements (i.e., γ_k) on the harvested power. As expected, the harvested power decreases with higher values of γ. This is due to the fact that the BS consumes more power to meet the SINR requirements, which results in a degradation of the total harvested power. An important observation is that there is a range of SINR for which the harvested energy remains more or less the same. However, with the increase of of SINR levels, the harvested power begins to drop significantly. Accordingly, the optimization problem OP_H tends to become infeasible due to insufficient power budget. With this trend, the harvested power settles down to zero, and we refer to this SINR requirement as γ^F. For example, as seen in Fig. 3, γ^F is 10 dB when $\mathrm{P}^A = 10$ dB, whereas it reaches 12 dB with $\mathrm{P}^A = 15$ dB.

To further understand the behaviour of OP_H with different SINR requirements, we provide more detailed results in Table 2. It can be observed that the users in the considered MISO-NOMA design can harvest power while meeting the minimum SINR requirements provided sufficient power budget is available at the BS. However, with higher SINR requirements and lower power budget P^A, the problem turns out to be infeasible as these requirements cannot be met with the available power budget. In this case, the BS alternatively chooses another option to maximize the sum rate of the system. Provided the original problem is infeasible, the users would be able to neither meet the SINR requirements nor the harvest the energy. Instead, the BS aims to maximize the sum rate of the system.

Furthermore, we investigate the impact of the users' distances on the harvested power. To study this impact, we fix the positions of the first and the second users, i.e., d_1 and d_2 at 20 meters and 30 meters, respectively, while the distance

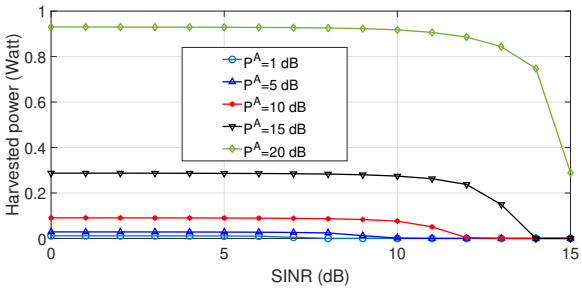

FIGURE 3: Harvested power versus different minimum SINR thresholds.

of the strongest user (i.e., d_3) is varied. The harvested power is evaluated with different values of d_3, as shown in Fig. 4. Note that the minimum distance of the strongest user in Fig. 4 is assumed to be 2 meters. In particular, the harvested power dramatically decreases with the increase of the strong user's distance. This is due to the fact that the increase of user's distance has a direct impact on the deterioration of its channel strength. Consequently, more power will be utilized by the strongest user to meet the corresponding minimum SINR requirement. As a result, this will degrade the corresponding amount of the harvested power. As evidenced in Fig. 4, with $\mathrm{P}^A = 10$ dB, the harvested power decays dramatically from around 2 Watts at a distance of 1 meter to less than 0.1 Watt at 15 meters. Moreover, at lower P^A levels, the increasing of distance makes OP_H infeasible, and thus, the harvested power approaches zero. For example, with $\mathrm{P}^A = 1$ dB, the harvested power becomes zero when the distance of the third user is larger than 4 meters.

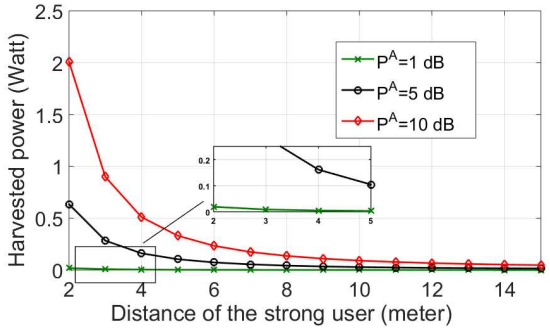

FIGURE 4: Harvested power versus the distance of the strong user for different available power budgets.

Next, we study the performance of the proposed SCA algorithm to solve the harvested power maximization problem OP_H. In Table 3, we provide the harvested power at the receiver of each user (i.e., $\mathrm{P}_i^H \ \forall i \in \{1,2,3\}$), the required transmit power, and the corresponding PS ratios obtained by solving OP_H via Algorithm 1 for a set of five random channels. In this simulation, we use the same design parameters in Table 2 to solve the power minimization problem $\approx{OP}_P$ via

TABLE 2: Harvested power, achieved rate, and PS ratio with different SINR requirements.

Available power	$P^A = 10$ dB			$P^A = 20$ dB		
Parameters \ SINR	γ=5 dB	γ=10 dB	γ=15 dB	γ=5 dB	γ=10 dB	γ=15 dB
R (Mbps)	5.4264	8.5895	11.9559	5.4362	9.1158	14.6196
P^H (Watt)	0.0902	0.0832	0	0.9293	0.9229	0.2890
β_1	0.0389	0.0287	1.0000	0.0015	0.0200	0.0798
β_2	0.0952	0.6874	1.0000	0.0220	0.0612	0.1151
β_3	0.0084	0.1561	1.0000	0.0014	0.0135	0.5468

TABLE 3: Power allocations and the power splitting ratios for different channels via solving OP_H with $P^A = 5$ dB.

USER	USER 1			USER 2			USER 3		
Parameters \ Channel	P_1 (Watt)	β_1	$P_{1,H}$ (Watt)	P_2(Watt)	β_2	$P_{2,H}$(Watt)	P_3(Watt)	β_3	$P_{3,H}$ (Watt)
Channel 1	8.2488	0.0018	0.0068	1.2825	0.0057	0.0171	0.4687	0.0022	0.0789
Channel 2	7.1811	0.0212	0.0008522	2.1370	0.0054	0.0101	0.6819	0.0015	0.0783
Channel 3	7.1925	0.0088	0.0021	2.1237	0.0066	0.0082	0.6837	0.0015	0.0780
Channel 4	7.7821	0.0054	0.0027	1.5554	0.0070	0.0123	0.6625	0.0015	0.0790
Channel 5	7.9333	0.0031	0.0045	1.4871	0.0056	0.0156	0.5797	0.0018	0.0783

SDP. The solutions of the P-Min problem $\widetilde{\approx}{OP}_P$ are included in Table 4. By drawing comparisons between the results presented in Tables 2 and 4, we conclude that both designs show similar results in terms of power allocations. This observation confirms that the proposed SCA algorithm is an efficient approach to jointly design beamforming vectors and PS ratios.

TABLE 4: Power allocations and the power splitting ratios obtained by solving $\widetilde{\approx}{OP}_P$ with $P^A = 5$ dB.

CHANNEL	P_1 (Watt)	P_2 (Watt)	P_3 (Watt)	Total power
Channel 1	8.2589	1.2800	0.4607	9.9995
Channel 2	7.1800	2.1453	0.6810	10.0064
Channel 3	7.1649	2.1611	0.6842	10.0102
Channel 4	7.7231	1.5963	0.6745	9.9938
Channel 5	7.9014	1.5258	0.5822	10.0094

Finally, we investigate the convergence of the proposed SCA algorithm in Fig. 5. In particular, we evaluate the convergence with the same set of five random channels considered in the previous simulations. As seen in Fig. 5, the proposed algorithm converges to the solution within a few number of iterations, i.e., less than 6 iterations.

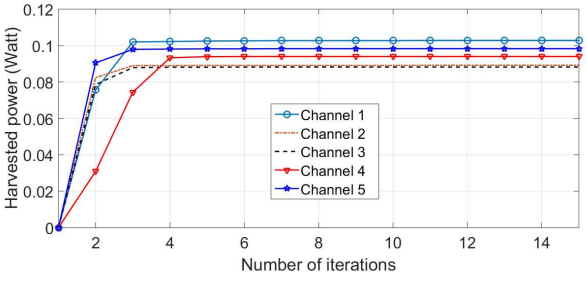

FIGURE 5: Convergence of the proposed algorithm when the available power P^A= 5 dB.

V. CONCLUSION

In this paper, we proposed a PS based SWIPT for MISO-NOMA system and provided an optimization technique for the joint design of the beamforming vectors and the corresponding PS ratios. To overcome the non-convexity issue of the original problem, an iterative algorithm was developed with the SCA approach. Furthermore, we devised systematic approaches to examine the feasibility, the convergence, and the evaluation of the proposed SCA algorithm. The simulation results confirmed that the MISO-NOMA system outperformed the conventional ZFBF based MISO system in terms of EH capability. We examined the impact of different system parameters on the harvested power. Furthermore, we showed that the proposed SCA technique obtains the solution of the problem with only a few number of iterations.

REFERENCES

[1] Y. Saito, Y. Kishiyama, A. Benjebbour, T. Nakamura, A. Li, and K. Higuchi, "Non-orthogonal multiple access (NOMA) for cellular future radio access," in *Proc. IEEE VTC Spring 2013*, pp. 1–5.

[2] S. Tomida and K. Higuchi, "Non-orthogonal access with SIC in cellular downlink for user fairness enhancement," in *Proc. IEEE Inter. Symp. on Intell. Signal Process. and Comm. Sys. (ISPACS), 2011*, pp. 1–6.

[3] S. Vanka, S. Srinivasa, Z. Gong, P. Vizi, K. Stamatiou, and M. Haenggi, "Superposition coding strategies: Design and experimental evaluation," *IEEE Trans. Wireless Commun.*, vol. 11, no. 7, pp. 2628–2639, Jul. 2012.

[4] X. Wei, H. Al-Obiedollah, K. Cumanan, M. Zhang, J. Tang, W. Wang, and O. A. Dobre, "Resource allocation technique for hybrid tdma-noma system with opportunistic time assignment," in *2020 IEEE International Conference on Communications Workshops (ICC Workshops)*. IEEE, 2020, pp. 1–6.

[5] H. Al-Obiedollah, "Resource allocation techniques for non-orthogonal multiple access systems," Ph.D. dissertation, University of York, 2019.

[6] Z. Ding, Y. Liu, J. Choi, Q. Sun, M. Elkashlan, I. Chih-Lin, and H. V. Poor, "Application of non-orthogonal multiple access in LTE and 5G networks," *IEEE Commun. Mag.*, vol. 55, no. 2, pp. 185–191, Feb. 2017.

[7] S. Riazul Islam, M. Zeng, O. A. Dobre, and K.-S. Kwak, "Non-orthogonal multiple access (noma): How it meets 5g and beyond," *arXiv preprint arXiv:1907.10001*, 2019.

[8] Z. Chen, Z. Ding, P. Xu, and X. Dai, "Optimal precoding for a QoS optimization problem in two-user MISO-NOMA downlink," *IEEE Commun. Lett.*, vol. 20, no. 6, pp. 1263–1266, Jun. 2016.

[9] M. Bashar, K. Cumanan, A. G. Burr, H. Q. Ngo, L. Hanzo, and P. Xiao, "On the performance of cell-free massive mimo relying on adaptive

noma/oma mode-switching," *IEEE Transactions on Communications*, vol. 68, no. 2, pp. 792–810, 2019.

[10] M. Zeng, A. Yadav, O. A. Dobre, and H. V. Poor, "Energy-efficient power allocation for mimo-noma with multiple users in a cluster," *IEEE Access*, vol. 6, pp. 5170–5181, 2018.

[11] Z. Ding, F. Adachi, and H. V. Poor, "The application of MIMO to non-orthogonal multiple access," *IEEE Trans. Wireless Commun.*, vol. 15, no. 1, pp. 537–552, Jan. 2016.

[12] F. Alavi, K. Cumanan, Z. Ding, and A. G. Burr, "Robust beamforming techniques for non-orthogonal multiple access systems with bounded channel uncertainties," *IEEE Commun. Lett.*, vol. 21, no. 9, pp. 2033–2036, Sept. 2017.

[13] Q. Sun, S. Han, I. Chin-Lin, and Z. Pan, "On the ergodic capacity of MIMO NOMA systems," *IEEE Wireless Commun. Lett.*, vol. 4, no. 4, pp. 405–408, Aug. 2015.

[14] L. Atzori, A. Iera, and G. Morabito, "The Internet of Things: A survey," *Comput. Netw.*, vol. 54, no. 15, pp. 2787–2805, Oct. 2010.

[15] P. Gandotra, R. K. Jha, and S. Jain, "Green communication in next generation cellular networks: a survey," *IEEE Access*, vol. 5, pp. 11 727–11 758, Jun. 2017.

[16] A. Zappone and E. Jorswieck, "Energy efficiency in wireless networks via fractional programming theory," *Found. Trends Commun. Inf. Theory*, vol. 11, no. 3-4, pp. 185–396, Jan. 2015.

[17] Y. Zhang, H.-M. Wang, T.-X. Zheng, and Q. Yang, "Energy-efficient transmission design in non-orthogonal multiple access," *IEEE Trans. Veh. Technol.*, vol. 66, no. 3, pp. 2852–2857, Mar. 2017.

[18] M. Zhang, K. Cumanan, J. Thiyagalingam, W. Wang, A. G. Burr, Z. Ding, and O. A. Dobre, "Energy efficiency optimization for secure transmission in miso cognitive radio network with energy harvesting," *IEEE Access*, vol. 7, pp. 126 234–126 252, 2019.

[19] L. R. Varshney, "Transporting information and energy simultaneously," in *Proc. IEEE ISIT 2008.*, 2008, pp. 1612–1616.

[20] W. Hao, G. Sun, F. Zhou, D. Mi, J. Shi, P. Xiao, and V. C. Leung, "Energy-efficient hybrid precoding design for integrated multicast-unicast millimeter wave communications with swipt," *IEEE Transactions on Vehicular Technology*, vol. 68, no. 11, pp. 10 956–10 968, 2019.

[21] X. Lu, P. Wang, D. Niyato, D. I. Kim, and Z. Han, "Wireless networks with RF energy harvesting: A contemporary survey," *IEEE Commun. Surveys Tuts.*, vol. 17, no. 2, pp. 757–789, Sec. quarter 2015.

[22] N. Zhao, S. Zhang, F. R. Yu, Y. Chen, A. Nallanathan, and V. C. Leung, "Exploiting interference for energy harvesting: A survey, research issues, and challenges," *IEEE Access*, vol. 5, pp. 10 403–10 421, May 2017.

[23] P. Xu and K. Cumanan, "Optimal power allocation scheme for non-orthogonal multiple access with α-fairness," *IEEE J. Sel. Areas in Commun.*, vol. 35, no. 10, pp. 2357–2369, Oct. 2017.

[24] I. Krikidis, S. Timotheou, S. Nikolaou, G. Zheng, D. W. K. Ng, and R. Schober, "Simultaneous wireless information and power transfer in modern communication systems," *IEEE Commun. Mag.*, vol. 52, no. 11, pp. 104–110, Nov. 2014.

[25] J. Huang, C.-C. Xing, and C. Wang, "Simultaneous wireless information and power transfer: Technologies, applications, and research challenges," *IEEE Communications Magazine*, vol. 55, no. 11, pp. 26–32, Nov. 2017.

[26] T. D. P. Perera, D. N. K. Jayakody, S. K. Sharma, S. Chatzinotas, and J. Li, "Simultaneous wireless information and power transfer (SWIPT): Recent advances and future challenges," *IEEE Commun. Surveys Tuts.*, vol. 20, no. 1, pp. 264–302, 1st Quart. 2017.

[27] H. Matsumoto and K. Hashimoto, "Report of the ursi inter-commission working group on sps and appendices," in *Solar Power Satellite Syst. Gen. Assembly Sci. Symp. Int. Union Radio Sci., Ghent, Belgium, White Paper*, 2006.

[28] A. Andrawes, R. Nordin, N. F. Abdullah *et al.*, "Energy-efficient downlink for non-orthogonal multiple access with swipt under constrained throughput," *Energies*, vol. 13, no. 1, pp. 1–19, Dec. 2019.

[29] J. Huang, C.-C. Xing, and C. Wang, "Simultaneous wireless information and power transfer: Technologies, applications, and research challenges," *IEEE Communications Magazine*, vol. 55, no. 11, pp. 26–32, 2017.

[30] Z. Goli, S. M. Razavizadeh, H. Farhadi, and T. Svensson, "Secure simultaneous information and power transfer for downlink multi-user massive mimo," *IEEE Access*, vol. 8, pp. 150 514–150 526, Aug. 2020.

[31] C. Pan, H. Ren, K. Wang, M. Elkashlan, A. Nallanathan, J. Wang, and L. Hanzo, "Intelligent reflecting surface aided mimo broadcasting for simultaneous wireless information and power transfer," *IEEE Journal on Selected Areas in Communications*, 2020.

[32] D. W. K. Ng, E. S. Lo, and R. Schober, "Robust beamforming for secure communication in systems with wireless information and power transfer," *IEEE Transactions on Wireless Communications*, vol. 13, no. 8, pp. 4599–4615, Apr. 2014.

[33] M. A. Hossain, R. M. Noor, K.-L. A. Yau, I. Ahmedy, and S. S. Anjum, "A survey on simultaneous wireless information and power transfer with cooperative relay and future challenges," *IEEE Access*, vol. 7, pp. 19 166–19 198, Jan. 2019.

[34] W. Hao, G. Sun, Z. Chu, P. Xiao, Z. Zhu, S. Yang, and R. Tafazolli, "Beamforming design in swipt-based joint multicast-unicast mmwave massive mimo with lens-antenna array," *IEEE Wireless Communications Letters*, vol. 8, no. 4, pp. 1124–1128, 2019.

[35] M. Vaezi, G. A. A. Baduge, Y. Liu, A. Arafa, F. Fang, and Z. Ding, "Interplay between NOMA and other emerging technologies: A survey," *IEEE Transactions on Cognitive Communications and Networking*, vol. 5, no. 4, pp. 900–919, Aug. 2019.

[36] J. Tang, J. Luo, M. Liu, D. K. So, E. Alsusa, G. Chen, K.-K. Wong, and J. A. Chambers, "Energy efficiency optimization for NOMA with SWIPT," *IEEE Journal of Selected Topics in Signal Processing*, vol. 13, no. 3, pp. 452–466, 2019.

[37] T.-V. Nguyen, V.-D. Nguyen, T.-N. Do, D. B. da Costa, and B. An, "Spectral efficiency maximization for multiuser MISO-NOMA downlink systems with SWIPT," in *Proc. IEEE Global Communications Conference (GLOBECOM)*, 2019, pp. 1–6.

[38] V.-D. Nguyen and O.-S. Shin, "An efficient design for NOMA-assisted MISO-SWIPT systems with AC computing," *IEEE Access*, vol. 7, pp. 97 094–97 105, July 2019.

[39] S. Mao, S. Leng, J. Hu, and K. Yang, "Power minimization resource allocation for underlay MISO-NOMA SWIPT systems," *IEEE Access*, vol. 7, pp. 17 247–17 255, Jan. 2019.

[40] Q. Qi, X. Chen, and D. W. K. Ng, "Robust beamforming for NOMA-based cellular massive IoT with SWIPT," *IEEE Trans. Signal Process.*, vol. 68, pp. 211–224, 2019.

[41] T. N. Do and B. An, "Optimal sum-throughput analysis for downlink cooperative SWIPT NOMA systems," in *Proc. IEEE 2nd SigTelCom, 2018*, pp. 85–90.

[42] Y. Liu, Z. Ding, M. Elkashlan, and H. V. Poor, "Cooperative non-orthogonal multiple access with simultaneous wireless information and power transfer." *IEEE J. Sel. Areas Commun.*, vol. 34, no. 4, pp. 938–953, Apr. 2016.

[43] Q. N. Le, A. Yadav, N.-P. Nguyen, O. A. Dobre, and R. Zhao, "Full-duplex non-orthogonal multiple access cooperative overlay spectrum-sharing networks with swipt," *IEEE Transactions on Green Communications and Networking*, Nov. 2020.

[44] G. L. Stuber, J. R. Barry, S. W. Mclaughlin, Y. Li, M. A. Ingram, and T. G. Pratt, "Broadband MIMO-OFDM wireless communications," *Proc. IEEE*, vol. 92, no. 2, pp. 271–294, Nov. 2004.

[45] Y. Dong, X. Ge, M. J. Hossain, J. Cheng, and V. C. Leung, "Proportional fairness-based beamforming and signal splitting for MISO-SWIPT systems." *IEEE Commun. Lett.*, vol. 21, no. 5, pp. 1135–1138, May 2017.

[46] A. Benjebbour, Y. Saito, Y. Kishiyama, A. Li, A. Harada, and T. Nakamura, "Concept and practical considerations of non-orthogonal multiple access (NOMA) for future radio access," in *Proc. IEEE Intell. Signal Process. and Commun. Syst. (ISPACS), 2013*, pp. 770–774.

[47] H. Al-obiedollah, K. Cumanan, J. Thiyagalingam, A. G. Burr, Z. Ding, and O. A. Dobre, "Sum rate fairness trade-off-based resource allocation technique for MISO NOMA systems," in *Proc. IEEE WCNC*, 2019.

[48] M. F. Hanif, Z. Ding, T. Ratnarajah, and G. K. Karagiannidis, "A minorization-maximization method for optimizing sum rate in the downlink of non-orthogonal multiple access systems," *IEEE Trans. Signal Process.*, vol. 64, no. 1, pp. 76–88, Jan. 2016.

[49] H. Zhang, K. Song, Y. Huang, and L. Yang, "Energy harvesting balancing technique for robust beamforming in multiuser MISO SWIPT system," in *Proc. IEEE International Conference on Wireless Communications & Signal Processing (WCSP)*, 2013, pp. 1–5.

[50] B. Khandaker and K.-K. Wong, "SWIPT in MISO multicasting systems," *IEEE Wireless Commun. Lett.*, vol. 3, pp. 277–280, Jun. 2014.

[51] H. Sun, F. Zhou, R. Q. Hu, and L. Hanzo, "Robust beamforming design in a NOMA cognitive radio network relying on SWIPT," *IEEE Sel. Areas in Commun.*, vol. 37, no. 1, pp. 142–155, Jan. 2019.

[52] E. Boshkovska, D. W. K. Ng, N. Zlatanov, A. Koelpin, and R. Schober, "Robust resource allocation for MIMO wireless powered communication networks based on a non-linear EH model," *IEEE Trans. Commun.*, vol. 65, no. 5, pp. 1984–1999, 2017.

[53] E. Boshkovska, D. W. K. Ng, N. Zlatanov, and R. Schober, "Practical non-linear energy harvesting model and resource allocation for SWIPT systems," *IEEE Commun. Lett.*, vol. 19, no. 12, pp. 2082–2085, 2015.
[54] H. Al-Obiedollah, K. Cumanan, J. Thiyagalingam, J. Tang, A. G. Burr, Z. Ding, and O. A. Dobre, "Spectral-energy efficiency beamforming design for MISO non-orthogonal multiple access systems," *IEEE Trans. Wireless Commun.*, Under Major revision.
[55] A. Beck, A. Ben-Tal, and L. Tetruashvili, "A sequential parametric convex approximation method with applications to nonconvex truss topology design problems," *J. Global Optimiz.*, vol. 47, no. 1, pp. 29–51, May 2010.
[56] F. Alavi, K. Cumanan, M. Fozooni, Z. Ding, S. Lambotharan, and O. A. Dobre, "Robust energy-efficient design for miso non-orthogonal multiple access systems," *IEEE Transactions on Communications*, vol. 67, no. 11, pp. 7937–7949, 2019.
[57] H. Al-obiedollah, K. Cumanan, J. Thiyagalingam, A. G. Burr, Z. Ding, and O. A. Dobre, "Energy efficiency fairness beamforming design for MISO NOMA systems," in *Proc. IEEE WCNC*, 2019.
[58] H. Al-Obiedollah, K. Cumanan, A. G. Burr, J. Tang, Y. Rahulamathavan, Z. Ding, and O. A. Dobre, "On energy harvesting of hybrid TDMA-NOMA systems," in *Proc. IEEE Globecom*, 2019.
[59] S. Boyd, S. P. Boyd, and L. Vandenberghe, *Convex optimization*. Cambridge university press, 2004.
[60] M. Bengtsson and B. Ottersten, "Optimal downlink beamforming using semidefinite optimization," in *Proc. Annual Allerton Conf. on Commun., Control and Computing*, 1999, pp. 987–996.
[61] F. Alavi, K. Cumanan, Z. Ding, and A. G. Burr, "Beamforming techniques for non-orthogonal multiple access in 5G cellular networks," *IEEE Trans. Veh. Technol.*, vol. 67, no. 10, pp. 9474–9487, Oct. 2018.
[62] L. Vandenberghe and S. Boyd, "Semidefinite programming," *SIAM review*, vol. 38, no. 1, pp. 49–95, 1996.
[63] M. Grant, S. Boyd, and Y. Ye, "CVX: Matlab software for disciplined convex programming," [Online]. Available: http://www.stanford.edu/boyd/cvx.